ISSN: 2710-0588

Design and Experimental Validation of an Automatic Inspection Robot Control System based on Multi-Sensor Fusion

Xiaodong Zhao[1], Yuxian Li[1], Hongwei Jiang[1], Fa Huang[1,2,*]

[1] Hebei University of Water Resources and Electric Engineering, Cangzhou 061016, China

[2] Hebei Industrial Manipulator Control and Reliability Technology Innovation Center, Cangzhou 061016, China

[*]Corresponding author Email: hangfa@hbwe.edu.cn

Abstract

To address the problems of high labor intensity, low efficiency, and safety risks in traditional manual inspection, as well as the insufficient environmental adaptability and limited path adjustment capability of existing inspection robots, an automatic inspection robot system based on multi-sensor fusion is designed. The system employs a Raspberry Pi 5 as the main control platform and integrates a Mecanum-wheel mobile mechanism, ultrasonic sensors, infrared sensors, and a camera pan-tilt module to accomplish the overall structural design, hardware selection, drive system development, and fusion control program implementation. In terms of software control, ultrasonic obstacle avoidance, infrared line tracking, and multi-sensor fusion decision-making functions are realized, and two operating modes, namely manual remote control and automatic inspection, are established. System debugging and experimental results demonstrate that the robot is capable of stable locomotion, path tracking, obstacle detection, and obstacle avoidance, thereby achieving the expected design objectives. The proposed system features a simple structure, low cost, convenient operation, and relatively stable performance, and can provide a useful reference for the design and application of low-cost intelligent inspection robots.

Keywords

Multi-Sensor Fusion, Inspection Robot, Ultrasonic Obstacle Avoidance, Infrared Line Tracking, Automatic Inspection.

1. Introduction

Operation and maintenance constitute a key measure for ensuring the safe and reliable operation of power systems [1]. For a long time, substation inspection tasks have mainly relied on manual work. However, with the rapid development of power systems, power grid companies are facing increasing pressure in inspection operations [2]. Meanwhile, the traditional manual inspection mode is characterized by high labor intensity, low inspection efficiency, high labor costs, and considerable safety risks, and can no longer meet the development needs of modern power systems [3].

Over the past decade, significant progress has been made in the research and application of inspection robots in China [4]. However, from the perspective of practical application, existing inspection robot systems still find it difficult to complete inspection tasks fully autonomously, mainly due to their insufficient autonomous navigation capability. For example, owing to the lack of high-precision local positioning functions, current substation inspection robots are unable to achieve accurate real-time localization and therefore can only conduct inspections along fixed routes [5]. In addition, because robots do not possess sufficient capability to interpret sensor information [6], even when road-environment data are acquired, they are

ISSN: 2710-0588

often unable to assess the current environment effectively. As a result, they usually move blindly according to maps, guide lines, or preset paths, rather than adjusting their behavior based on real-time road conditions. When unexpected situations arise, manual intervention is often required, indicating inadequate autonomous emergency-handling capability. With the rapid advancement of network communication technology, information processing technology, artificial intelligence, big data technology, navigation technology, and power electronics [7], the use of multi-sensor fusion-based automatic inspection robots to replace traditional manual inspection has become an effective solution to these problems.

The significance of this study is mainly reflected in three aspects: reducing labor costs, lowering safety risks, and improving inspection efficiency. First, replacing traditional manual inspection with a multi-sensor fusion-based automatic inspection robot can reduce dependence on human labor and avoid constraints imposed by time, weather, and other external factors, thereby lowering labor and time costs. Second, equipped with infrared and ultrasonic obstacle avoidance systems, the robot can avoid hazardous equipment and harmful environments, significantly reducing operational safety risks. Third, compared with manual inspection, whose efficiency is easily affected by fatigue and environmental conditions, the robot can rapidly and accurately identify equipment problems, eliminating the need for extensive manual analysis and substantially improving inspection efficiency and accuracy.

2. Design of the Robot Locomotion Mechanism

The working environment of automatic inspection robots is often highly complex, such as substations, underground pipelines, and factory workshops [8]. These environments are generally characterized by narrow spaces, uneven ground surfaces, and, in some cases, scattered obstacles or debris. Therefore, robots operating in such scenarios require agile mobile mechanisms. In addition, these environments are often subject to various types of interference, including electromagnetic waves generated by operating machinery, airborne dust, and fluctuating lighting conditions. Under such circumstances, conventional sensors may produce errors and inaccurate measurements. For this reason, multiple types of sensors need to be integrated into the robot system so that they can operate cooperatively. For example, LiDAR can be used for contour detection, cameras for object recognition, ultrasonic sensors for distance measurement, and infrared sensors for line tracking. In this way, even if one sensor fails, the system can still maintain stable operation.

Common mobile mechanisms for inspection robots include tracked, legged, wheel-track hybrid, magnetic adhesion, rail-guided, and wheeled types [9,10]. Among them, tracked mechanisms are suitable for rough and loose terrain, offering good obstacle-crossing capability, but they generally have low movement speed, relatively high maintenance costs, and moderate control complexity. Legged mechanisms, based on tracked systems, are even more suitable for extreme terrain conditions; however, they move more slowly and involve extremely high control complexity and cost. Wheel-track hybrid mechanisms can adapt to mixed terrains, but their control is also relatively complex. Magnetic adhesion and rail-guided mechanisms both require specific operating environments and preset paths, which reduces their obstacle-crossing capability [11]. Rail-guided systems are easy to control but usually have high energy consumption, whereas magnetic adhesion systems are difficult to control, move slowly, and incur high maintenance costs. By contrast, wheeled mechanisms are suitable for flat and hardened ground surfaces. They are easier to control and can achieve higher speeds, making them more appropriate for environments such as power plants, where the ground is generally flat and equipment is densely distributed. A comparison of common mobile mechanisms is shown in Table 1.

ISSN: 2710-0588

Table 1. Comparison Table of Commonly Used Mobile Mechanisms

Mobile Mechanism	Obstacle-Crossing Ability	Movement Speed	Control Complexity	Energy Efficiency
Wheeled	Weak	Fast	Low	High
Tracked	Medium	Moderate	Moderate	Moderate
Legged	Strong	Slow	Very high	Very low
Wheel-track hybrid	Medium to strong	Moderately fast	High	Moderate
Magnetic adhesion	None	Slow	High	Moderate
Rail-guided	None	Stable	Very low	Very high

Considering that inspection environments usually involve challenges such as narrow passages, complex terrain, and obstacles, conventional wheeled structures, although simple in design and convenient to control, generally exhibit poor passability in complex terrains and are particularly prone to being trapped when encountering trenches or steps. However, the Mecanum wheel, as an omnidirectional mobile mechanism, employs a special roller arrangement on four wheels [12], enabling all-directional motion, including forward and backward movement, lateral translation, diagonal motion, and in-place rotation. This effectively overcomes the drawback of traditional wheeled mechanisms, which often require repeated adjustments in complex environments such as L-shaped passages.

A Mecanum wheel consists of a hub and a set of rollers distributed around the hub. These rollers are passive and non-driven small rollers. The angle between the roller axis and the hub axis is 45°, and there are two mirrored wheel types, commonly referred to as Type A and Type B wheels, or alternatively as left-handed and right-handed wheels. The outer rollers of the Mecanum wheel are in contact with the ground. When the wheel rotates about the hub axis, friction is generated between the rollers and the ground. This ground friction can be decomposed into components perpendicular and parallel to the roller axis. Among them, the component perpendicular to the roller axis corresponds to rolling friction, which drives the rollers to rotate and is therefore regarded as ineffective motion. In contrast, the component parallel to the roller axis corresponds to static friction, which causes the rollers to move relative to the ground and thereby drives the entire Mecanum wheel to move along the roller axis.

For the kinematic analysis, the robot velocity vector can be expressed as $V = [v_x,\ v_y,\ \omega]^T$, where v_x is the velocity along the X-axis, v_y is the velocity along the Y-axis, and ω is the angular velocity of the robot body. Their relationship with the rotational speeds of the four wheels, denoted by $\omega_1,\ \omega_2,\ \omega_3,\ \omega_4$ is given in Eq. (1):

$$\begin{bmatrix}\omega_1\\ \omega_2\\ \omega_3\\ \omega_4\end{bmatrix} = \frac{1}{r}\begin{bmatrix}1 & -1 & -(l_x+l_y)\\ 1 & 1 & (l_x+l_y)\\ 1 & 1 & -(l_x+l_y)\\ 1 & -1 & (l_x+l_y)\end{bmatrix}\begin{bmatrix}v_x\\ v_y\\ \omega\end{bmatrix} \tag{1}$$

where r is the radius of the wheel, l_x is the distance from the wheel center to the geometric center of the robot along the X-axis, and l_y is the distance from the wheel.center to the geometric center of the robot along the Y-axis. In addition, the overall motion state of the robot can also be inversely determined from the wheel speeds by calculating the inverse of the corresponding transformation matrix.The torque of each wheel, denoted by τ_i, must overcome

ISSN: 2710-0588

rolling resistance, acceleration, and ground friction. The corresponding relationship is given in Eq. (2).

$$\tau_i = r \cdot \left(F_{roll} + F_{accel} + F_{friction}\right) \tag{2}$$

3. Sensor Configuration of the Automatic Inspection Robot

The core requirements of sensors for automatic inspection robots are mainly reflected in the comprehensiveness and reliability of environmental perception [13]. The robot must be capable of accurately perceiving the distance, position, and characteristics of surrounding obstacles, while also adapting to complex environmental factors such as varying lighting conditions and changes in temperature and humidity. In addition, considering the continuity of inspection tasks, the power consumption and stability of sensors are also important factors. Under the premise of controllable cost, achieving effective fusion of multi-source information is the key to improving overall system performance.

Common sensors used in multi-sensor fusion-based automatic inspection robots include LiDAR, vision sensors, ultrasonic sensors, infrared sensors, gas sensors, temperature and humidity sensors, and acoustic sensors [14].

Ultrasonic sensors measure nearby obstacles based on the principle of sound-wave reflection. They have the advantages of low cost and strong anti-interference capability, and are commonly used for short-range obstacle avoidance and auxiliary positioning. They can also be used redundantly with LiDAR or vision sensors to perform close-range obstacle avoidance. Considering their low cost and simple control, ultrasonic sensors were selected as one type of sensor in this design.

Infrared sensors are commonly used for path tracking [15]. Based on the reflective characteristics of infrared light, they emit infrared signals and receive the reflected light. The intensity of the received infrared signal is then converted into different electrical signals to achieve line-tracking functionality. Infrared sensors can work cooperatively with ultrasonic sensors to realize specific path tracking and obstacle avoidance. Owing to their low cost and relatively simple control, infrared sensors were also selected as a sensor type in this design.

Under the complex operating conditions of power plants, automatic inspection robots face many special challenges, including narrow equipment spacing, complicated metallic structural environments, electromagnetic interference, and variations in temperature and humidity. These characteristics impose stringent requirements on sensor selection, which must simultaneously consider measurement accuracy, environmental adaptability, and system reliability. Through in-depth analysis and comparison of various sensor types, this study finally determined a technical scheme integrating ultrasonic obstacle-avoidance sensors and infrared line-tracking sensors. The fusion of these two sensors enables multi-dimensional environmental perception: the ultrasonic sensor is responsible for three-dimensional safety monitoring, while the infrared sensor ensures accurate planar navigation during robot movement.

4. Multi-Sensor Fusion Control Method

In the complex inspection environment of power plants, there are various types of equipment of different sizes. Within the narrow spaces between these devices, the inspection robot is required to move flexibly in order to detect potential problems. Owing to the particular characteristics of on-site operating conditions, the robot should be capable of both manual and automatic control modes. When abnormal equipment movement occurs or when sensors fail due to strong electromagnetic interference, operation and maintenance personnel can use the

ISSN: 2710-0588

manual mode to carry out close-range inspection and safe obstacle avoidance. In contrast, the automatic mode can accomplish inspection tasks more efficiently and reduce labor costs. Based on these considerations, this chapter presents the program design for both manual and automatic modes. Combined with the selected vision-based robotic vehicle platform, the system can realize safe obstacle avoidance, path tracking, and visual observation and detection functions.

4.1. Ultrasonic Obstacle Avoidance

The ultrasonic sensor measures distance based on the time difference of sound-wave reflection. Specifically, the sensor emits high-frequency sound waves, which propagate through the air and are reflected when they encounter an obstacle. The reflected waves are then received by the sensor, and the distance is calculated according to the time interval between sound-wave transmission and reception, together with the speed of sound. The specific formula is given in Eq. (3).

$$d = \frac{v \times \Delta t}{2} \tag{3}$$

where d is the measured distance, in meters; v is the speed of sound, which is approximately 343 m/s at room temperature; and t is the time interval between ultrasonic wave transmission and reception, in seconds. Under the complex operating conditions of power plants, including strong electromagnetic interference, fluctuations in temperature and humidity, and dense metallic equipment, the HC-SR04 ultrasonic module (as shown in Fig. 1) was selected because of its strong anti-interference capability, as its 40 kHz ultrasonic waves are not affected by electromagnetic fields, its wide environmental adaptability, and its favorable reflective performance on metallic surfaces, with a reflectivity of 92% for stainless steel. Its detection range of 2 cm to 4 m matches the safety clearance requirements of equipment inspection, and its repeatability of 3 mm satisfies the accuracy requirements of power inspection tasks.

Fig. 1 HC-SR04 Ultrasonic Module

The ultrasonic obstacle-avoidance program is designed as follows. The parameter NEAR_DISTANCE is set to 200 mm, and FAR_DISTANCE is set to 425 mm. When the detected distance is less than 200 mm, the robot moves backward for 0.1 s. When the detected distance is between 200 mm and 425 mm, the robot first stops for 0.2 s and then turns left for 0.15 s. When the detected distance is greater than 425 mm, the robot moves forward.

After that, the main program is executed to activate the ultrasonic ranging function, and the obstacle-avoidance logic runs continuously in a loop. Functions provided by the robot drive library, such as move_forward and move_backward, are used to control the motion of the robot, while the time.sleep() function is employed to precisely control the duration of each action. In

ISSN: 2710-0588

the event of an exception, the program can be interrupted by pressing Ctrl+C, which disables the ultrasonic function and stops the robot.The specific performance is shown in Fig. 2.

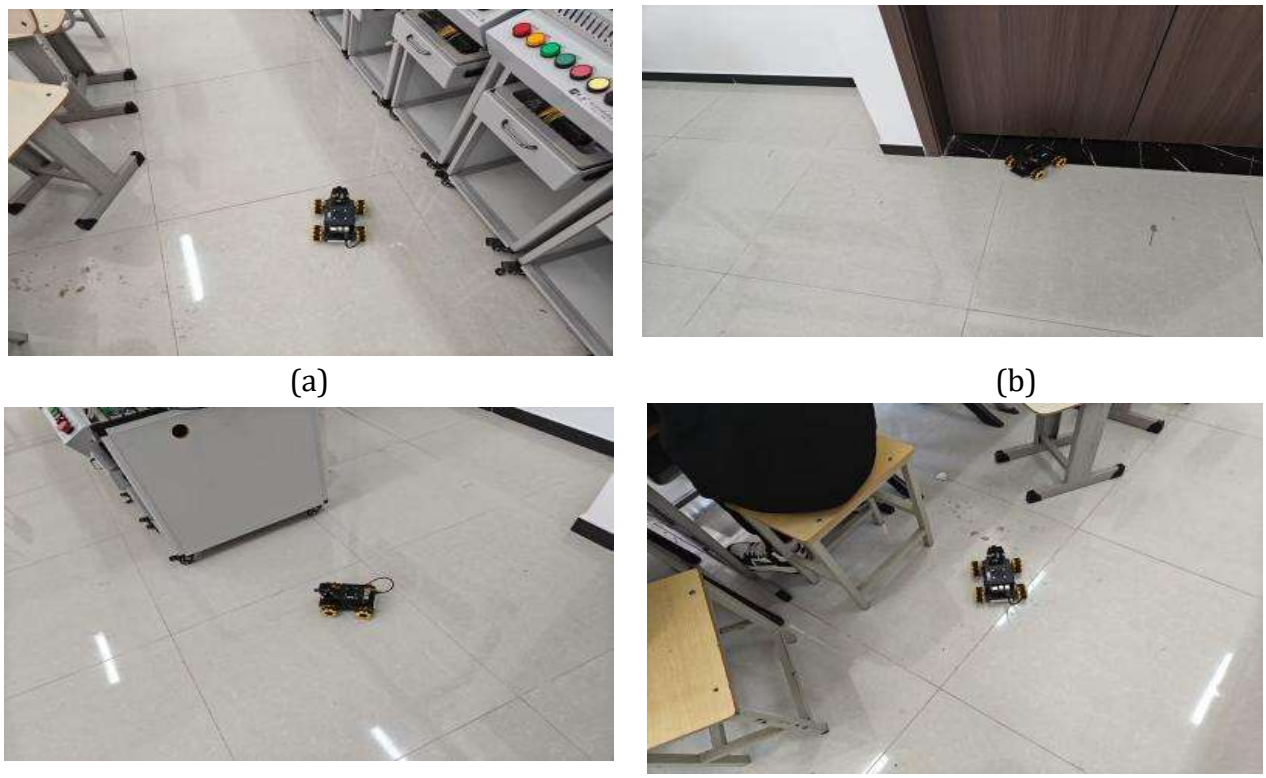

(a) (b)

(c) (d)

Fig. 2 The ultrasonic obstacle-avoidance behavior of the robot is illustrated

4.2. Infrared Line-Tracking Program

The core of infrared line tracking lies in infrared reflective photoelectric detection. The infrared line-tracking sensor emits infrared light toward the ground and receives the reflected signal from the surface. The black tracking path absorbs most of the infrared light and therefore produces weak reflection, causing the sensor to output a low-level signal. In contrast, the light-colored area outside the tracking path reflects more infrared light, resulting in strong reflection and thus a high-level sensor output. The relationship between the reflected light intensity and the distance is given in Eq. (4).

$$I_r = I_o \cdot e^{-\alpha d} \cdot R \tag{4}$$

Under the complex ground conditions of power plants, including metal gratings, epoxy floors, and oil contamination, the TCRT5000 infrared line-tracking module (as shown in Fig. 3) was selected because of its dual digital/analog output modes, detection accuracy of ±1 mm, 38 kHz modulated anti-light-interference capability, and IP42 protection rating, which enable stable identification of ground features with different reflectivities. Its compact design supports four-channel cooperative detection, and, with the aid of an adaptive threshold algorithm, it can effectively overcome the interference caused by common ground stains in power plants. Compared with conventional photoelectric switch solutions, it provides better line-tracking smoothness and environmental adaptability. Experimental results show that the path-tracking deviation is less than ±2 mm, which satisfies the high-precision navigation requirements of power equipment inspection.

ISSN: 2710-0588

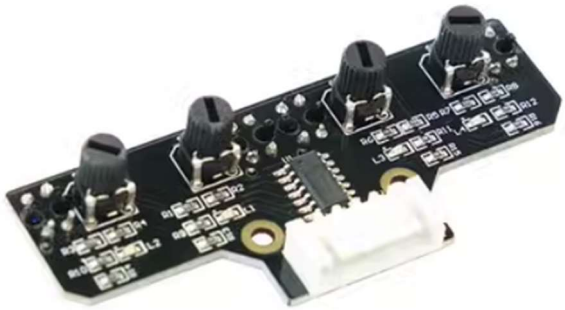

Fig. 3 Four-Channel TCRT5000 Infrared Line-Tracking Module

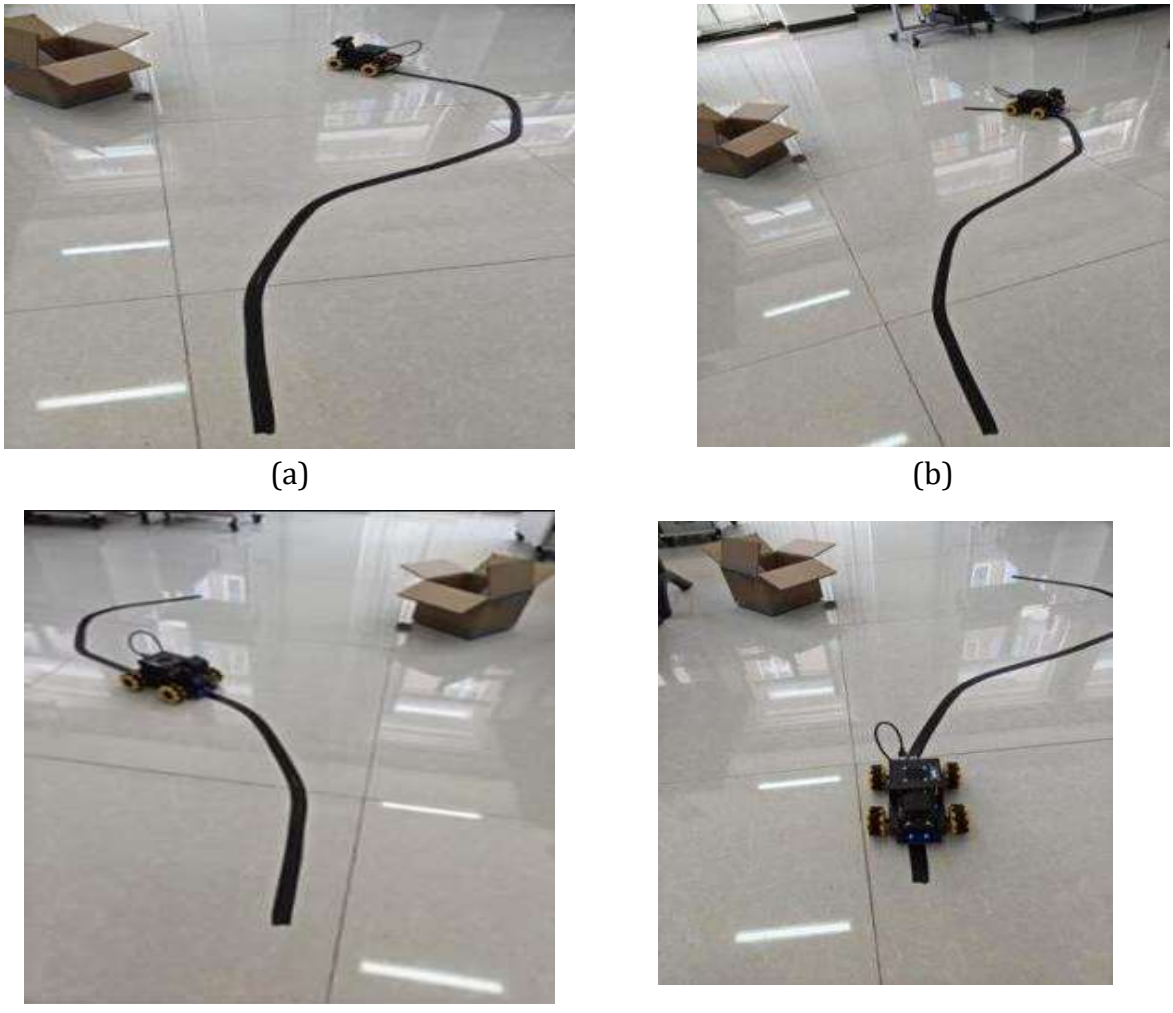

(a) (b)

(c) (d)

Fig. 4 Infrared Line-Tracking Performance of the Robot

The designed program realizes automatic black-line following by reading the infrared line-tracking sensor data through the I2C interface, determining the position of the robot relative to the black line, and adjusting the robot's motion direction according to different conditions. The core logic of the program lies in the interpretation and processing of sensor data. The sensor consists of four infrared probes, namely the left outer probe (L1), left inner probe (L2), right inner probe (R1), and right outer probe (R2), which are arranged in a straight line. When a probe detects the black line, it outputs a low-level signal (0); when it detects the white

ISSN: 2710-0588

background, it outputs a high-level signal (1). The program reads the combined states of these four probes as one byte of data and uses bitwise operations to decode the status of each probe.

The program uses the time.sleep() function to control the time interval between each detection and adjustment, ensuring that the system has sufficient time to respond and execute the corresponding actions. At the same time, an exception-handling mechanism is implemented, allowing the program to be interrupted by pressing Ctrl+C, which immediately stops all robot motions to ensure operational safety. The specific performance is shown in Fig. 4.

4.3. Multi-Sensor Fusion Motion Control Program

There are four common types of multi-sensor fusion. The first is complementary fusion, in which sensors operate independently and cover different perceptual dimensions. For example, a camera and a LiDAR sensor can be combined, with the camera providing color and texture information and the LiDAR providing accurate distance measurements. The advantage of this approach lies in expanding the perception range and improving system robustness. The second type is redundant fusion, which refers to cross-validation using multiple sensors of the same type. A typical example is binocular stereo vision, where two cameras are used to calculate depth through disparity. Its main advantage is the reduction of false detections and the improvement of fault tolerance. The third type is cooperative fusion, in which multiple sensors jointly solve tasks that cannot be accomplished by a single sensor alone. For instance, infrared and visible-light cameras can be combined for all-weather target tracking. The advantage of this method is that it enhances perception capability and can achieve a “1 + 1 > 2” effect. The fourth type is hierarchical fusion, in which sensor data are processed according to priority levels. For example, in emergency obstacle avoidance, ultrasonic sensor data are processed before visual information. The advantage of this hierarchical strategy is that it optimizes the allocation of computational resources.

The fusion logic adopted in this design combines ultrasonic obstacle avoidance and infrared line tracking, which can be regarded as a form of cooperative fusion with hierarchical priority. After the robot system is started, the robot moves forward along the black line and adjusts its direction according to the infrared sensor signals. Meanwhile, the ultrasonic sensor detects whether there is an obstacle ahead and determines whether the measured distance is less than 200 mm. If the distance is below this threshold, the robot stops and continuously issues an alarm until the obstacle is removed, after which it resumes moving forward along the black line. If the distance is greater than 200 mm, the robot continues line tracking without interruption.

To implement the proposed multi-sensor fusion program, the library file path is first added and the Mecanum-wheel robot drive library is imported. The default speed is then set to 30, and the ultrasonic ranging function is activated. After that, the program enters the main loop and continuously executes the line-tracking and obstacle-avoidance logic. The line-tracking sensor data are read from the I2C address 0x0a, converted into integers, and then decoded through bitwise operations to determine the states of the four infrared sensors. Meanwhile, the ultrasonic distance data are read from two I2C registers, corresponding to the high byte and low byte, and combined into a complete distance value.

If the detected obstacle distance is less than 200 mm, the robot stops and activates the buzzer alarm for 0.1 s, after which the buzzer is turned off. If no obstacle is detected, the program executes eight line-tracking control rules. In the first case, when none of the sensors detects the black line (0000), the robot accelerates forward. In the second case, when the left one or two sensors and the right outer sensor detect the black line, the robot performs a relatively large right turn. In the third case, when the left outer sensor and the right one or two sensors detect the black line, the robot makes a sharp left turn. In the fourth case, when only the left outermost sensor L1 detects the black line, the robot performs a slight left adjustment. In the fifth case, when only the right outermost sensor R2 detects the black line, the robot performs a slight right

ISSN: 2710-0588

adjustment. In the sixth case, when the left inner sensor detects the black line while the right inner sensor does not, the robot performs a slight left correction. In the seventh case, when the right inner sensor detects the black line while the left inner sensor does not, the robot performs a slight right correction. In the eighth case, when the two middle sensors simultaneously detect the black line, the robot maintains straight-line motion. If an exception occurs, the ultrasonic ranging function can be disabled and all motors can be stopped immediately by pressing Ctrl+C. The specific performance is shown in Fig. 5.

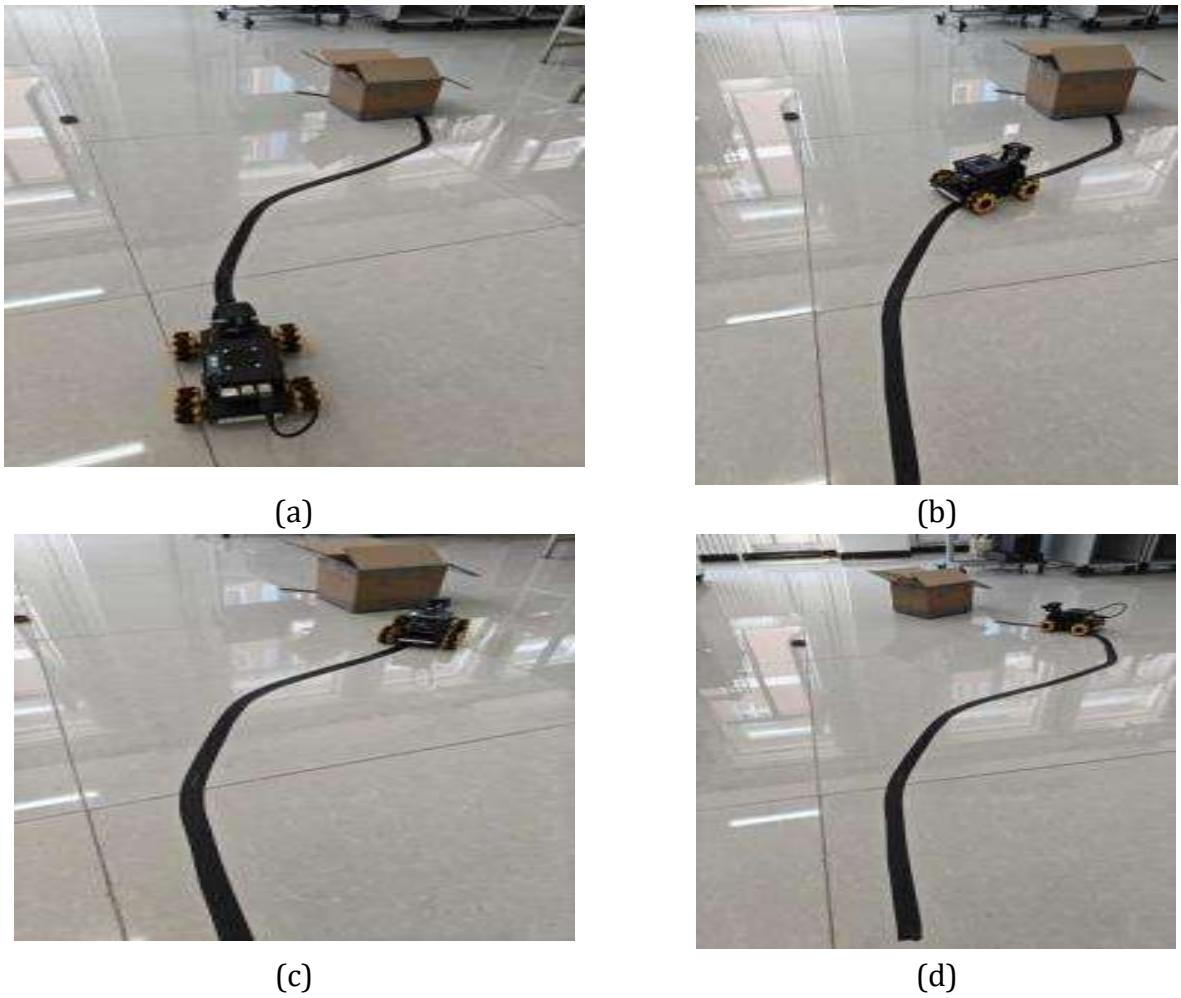

(a) (b)

(c) (d)

Fig. 5 Experimental results of the overall fusion program of the car

The overall fusion program operated well. Occasionally, slight path deviations occurred due to excessive speed, but the test results remained unchanged. The debugging results met expectations, demonstrating that the system can achieve efficient automatic inspection in the narrow, multi-equipment environment of a power plant.

5. Summary

With the continuous development of modern power systems, traditional manual inspection methods have gradually revealed a number of shortcomings, including high labor intensity, low inspection efficiency, high labor costs, and significant safety risks. Meanwhile, automatic inspection robots have been increasingly and widely applied in various types of power plants due to their advantages in intelligence, automation, and strong environmental adaptability. Therefore, this study focuses on the design of the control system for a multi-sensor fusion-

ISSN: 2710-0588

based automatic inspection robot, with the aim of enabling the vehicle to perform autonomous mobile inspection in electrical equipment environments.

The main work completed in this study is as follows:

(1) The overall selection and design of the hardware system for the intelligent inspection vehicle were completed. Through a comprehensive comparison of multiple schemes, the Raspberry Pi 5 was ultimately selected as the control core of the intelligent inspection vehicle, Mecanum wheels were adopted as the mobile mechanism, and a two-degree-of-freedom camera gimbal was employed as the visual actuation unit, thereby providing the hardware foundation for motion control and environmental perception of the system;

(2) The design and programming of the software control programs for each subsystem were completed, mainly including the ultrasonic obstacle avoidance program, the four-channel infrared line-tracking program, the low-level driver program, and the multi-sensor fusion control program, thus realizing functions such as path recognition, obstacle avoidance, motion control, and multi-source information collaborative processing;

(3) The construction of the physical prototype and the experimental testing were finally completed. The system successfully achieved the organic integration of two control modes, namely manual operation and automatic line-tracking with obstacle avoidance, while also enabling both independent sensor operation and multi-sensor fusion operation. The experimental results indicate that the system possesses good environmental adaptability, control stability, and cooperative perception capability, thereby laying a solid foundation for subsequent engineering application.

Acknowledgments

This work was financially supported by The College Students' Innovation and Entrepreneurship Training Program Project(S202410085051) fund.

References

[1] Zhao Zukang, Xu Shiming. Review of substation automation technology. Electric Power Automation Equipment. No. 1 (2000), p. 40-44.

[2] Song Xuankun, Yan Peili, Wu Lei, et al. Review of key technologies in pilot projects of smart substations. Electric Power Construction. Vol. 34 (2013) No. 7, p. 10-16.

[3] Li Jian, Li Xudong, Du Lin, et al. An intelligent sensor for the ultra-high-frequency partial discharge online monitoring of power transformers. Energies. Vol. 9 (2016) No. 5, p. 20-26.

[4] Yang Xudong, Huang Yuzhu, Li Jigang, et al. Review of research on substation inspection robots. Shandong Electric Power Technology. Vol. 42 (2015) No. 1, p. 30-34.

[5] Tang Xu. Research on visual navigation and path planning of substation inspection robot (Master's thesis, Yangzhou University, China, 2015).

[6] Lin Chao, Dai Hao, Xue Zhicheng, et al. Review on the application of intelligent inspection robots in substations. Automation Application. No. 12 (2018), p. 73-75.

[7] Yang Fan. Development status and prospects of unmanned vehicles. Shanghai Auto. No. 3 (2014), p. 35-40.

[8] Beşdok Erkan. 3D vision by using calibration pattern with inertial sensor and RBF neural networks. Sensors. Vol. 9 (2009) No. 6, p. 6.

[9] Lu Shouyin, Qian Qinglin, Zhang Bin, et al. Development of substation equipment inspection robot. Automation of Electric Power Systems. No. 13 (2006), p. 94-98.

[10] Campsite under the visual field of low-carbon environmental protection. Advanced Materials Research. Vol. 573 (2012), p. 1320.

ISSN: 2710-0588

[11] Ozawa Masaki, Okada Yoshito, Tadakuma Kenjiro. Robot system for inspecting inner wall of large boiler. Proceedings of the JSME Annual Conference on Robotics and Mechatronics (ROBOMEC). Japan, 2017, p. 9-17.

[12] Lee Jisun, Kwon Jay Hyoun, Yu Myeongjong. Performance evaluation and requirements assessment for gravity gradient referenced navigation. Sensors. Vol. 15 (2015) No. 7, p. 75-98.

[13] Masmoudi Mohamed Slim, Krichen Najla, Masmoudi Mohamed, et al. Fuzzy logic controllers design for omnidirectional mobile robot navigation. Applied Soft Computing. Vol. 49 (2016), p. 5-9.

[14] Yang Sijie. Analysis of key technologies of substation inspection robot. Wireless Internet Technology. Vol. 16 (2019) No. 1, p. 136-137.

[15] Xiao Peng, Sun Daqing, Wang Mingrui, et al. Design of navigation system for intelligent substation inspection robot based on laser positioning. Computer Measurement & Control. Vol. 20 (2012) No. 6, p. 1629-1635.